JCI The Journal of Clinical Investigation

G-CSF resistance of *ELANE* mutant neutropenia depends on SERF1 containing truncated neutrophil elastase aggregates

Ramesh C. Nayak, … , Carolyn Lutzko, Jose A. Cancelas

J Clin Invest. 2024. https://doi.org/10.1172/JCI177342.

Research In-Press Preview Hematology

Graphical abstract

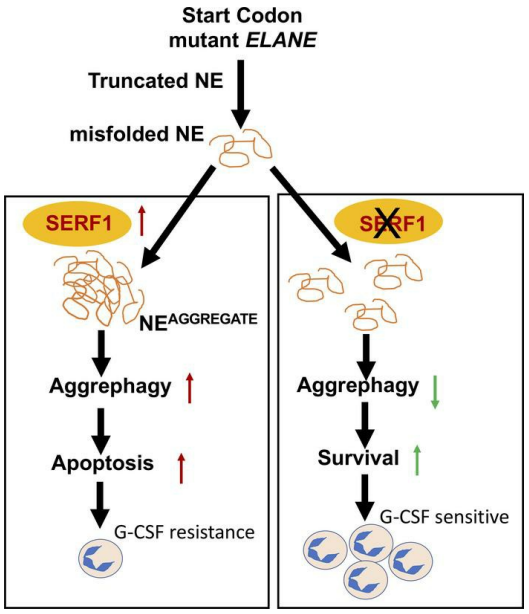

G-CSF resistance of *ELANE* mutant neutropenia depends on SERF1 containing truncated neutrophil elastase aggregates

Nayak, R.C.[1], Emberesh S.[2], Trump L.R. [2], Wellendorf A.M.[2], Singh A.K. [1], Korkmaz, B.[3], Horwitz M.S.[4], Myers, K.C.[2], Kalfa T.A.[2], Lutzko C.M.[1,2], Cancelas J.A.[1,2,5]

1. Hoxworth Blood Center, University of Cincinnati College of Medicine, Cincinnati, OH
2. Cancer & Blood Diseases Institute, Cincinnati Children's Hospital Medical Center, University of Cincinnati College of Medicine, Cincinnati, OH
3. INSERM UMR-1100, Research Center for Respiratory Diseases, and University of Tours, Tours, France.
4. Department of Laboratory Medicine & Pathology, University of Washington School of Medicine, Seattle, WA
5. Connell and O'Reilly Families Cell Manipulation Core Facility & Department of Medical Oncology, Dana-Farber Cancer Institute, Harvard Medical School, Boston, MA

Correspondence should be sent to:

Ramesh C. Nayak, PhD
Hoxworth Blood Center
University of Cincinnati College of Medicine
3130 Highland Ave.,
Cincinnati, OH, 45219
Tel: 513-558-1201
E-mail: Ramesh.Nayak@uc.edu

and

Jose A. Cancelas MD, PhD
Connell and O'Reilly Families Cell Manipulation Core Facility &
Department of Medical Oncology
Dana-Farber Cancer Institute
Harvard Medical School
450 Brookline Ave.
Boston, MA, 02215
Tel: 617-632-3446
E-mail: jose_cancelas-perez@dfci.harvard.edu

Running title

Aggrephagy in G-CSF resistant SCN

Abstract

Severe congenital neutropenia (SCN) is frequently associated with dominant point mutations in *ELANE*, the gene encoding neutrophil elastase (NE). Chronic administration of granulocyte colony-stimulating factor (G-CSF) is a first-line treatment of *ELANE*-mutant (*ELANE*^{mut}) SCN. However, some *ELANE*^{mut} patients including patients with *ELANE* start codon mutations do not respond to G-CSF. Here, through directed granulopoiesis of gene-edited isogenic normal and patient-derived iPSCs, we demonstrate that *ELANE* start codon mutations suffice to induce G-CSF resistant granulocytic precursor cell death and refractory SCN. *ELANE* start codon mutated neutrophil precursors express predominantly nuclear N-terminal truncated alternate NE. Unlike G-CSF sensitive *ELANE* mutations that induce endoplasmic reticulum and unfolded protein response stress, we found that the mutation of the *ELANE* translation initiation codon resulted in NE aggregates and activated pro-apoptotic aggrephagy as determined by downregulated BAG1 expression, decreased BAG1/BAG3 ratio, NE co-localization with BAG3, and localized expression of autophagic LC3B. We found that SERF1, an RNA-chaperone protein, known to localize in misfolded protein aggregates in neurodegenerative diseases, was highly upregulated and interacted with cytoplasmic NE of mutant neutrophil precursors. Silencing of SERF1 enhanced survival and differentiation of iPSC-derived neutrophil precursors, restoring their responsiveness to G-CSF. These observations provide a mechanistic insight of G-CSF-resistant *ELANE*^{mut} SCN, revealing targets for therapeutic intervention.

Brief Summary

Start codon mutations of *ELANE* result in aggregates of truncated NE that activate aggrephagy and induce resistance to G-CSF, reversible by silencing SERF1.

Introduction

Germline heterozygous point mutations in the gene *ELANE* are the most frequent cause of severe congenital neutropenia (SCN). SCN results from cell death and maturation arrest of bone marrow neutrophil precursors (1-4). Although, granulocyte colony-stimulating factor (G-CSF) administration increases peripheral blood (PB) neutrophil counts (ANC) in most *ELANE*^{mut} SCN patients(5), patients with mutations involving the translation initiation codon of the *ELANE* gene are resistant to G-CSF administration (6-8). Moreover, up to a quarter of *ELANE*^{mut} SCN cases on long-term, high-dose G-CSF therapy develop somatic CSF3R activating mutations preceding the onset of MDS/AML (9), underscoring the need to investigate alternative combinatorial therapies that could decrease therapeutic reliance on G-CSF.

The pathogenesis of many cases of *ELANE*^{mut} SCN pivots around mislocalization, impaired endoplasmic reticulum (ER) trafficking of mutant NE, and induction of unfolded protein response (UPR) pathways that leads to death and differentiation arrest of neutrophilic precursors (2, 10, 11). Earlier, we have shown that mutation at the translation initiation codon of *ELANE* results in alternate NE (N-terminal truncated) expression translating from downstream in-frame start codons (12). However, the molecular and cellular mechanisms of the pathogenesis and G-CSF resistance of *ELANE* translation initiation codon mutant SCN has been largely unknown.

In this study, we modeled G-CSF-resistant SCN associated with *ELANE* translation initiation codon mutations using patient-derived and gene-edited iPSCs. We found that the mutation at the *ELANE* translation initiation codon results in expression and aggregation of N-terminal truncated alternate NE peptides, induction of exaggerated aggrephagy along with upregulation of SERF1. We showed that downregulation of SERF1 prevents aggregate formation and rescues granulocytic precursor survival and differentiation. Our study illustrates an alternate mechanism of protein aggregation-mediated pathobiology of *ELANE* translation initiation codon mutant SCN.

Results

ELANE translation initiation codon mutation induces apoptosis and impairs differentiation.

In the present study, we modeled and investigated the mechanisms underlying G-CSF-resistant SCN pathobiology with mutations at the translation initiation codon of *ELANE*. We reprogrammed iPSC from PB mononuclear cells (MNC) of healthy subjects (normal*)* and two SCN subjects (GTG-P1 and GTG-P2) with heterozygosity for *ELANE* c.1A>G, p.(M1V) and *ELANE* c.3G>A, p.(M1I), respectively. As illustrated in Figure 1A, SCN patient 1, who donated the source cells to generate GTG-P1 iPSC did not respond to G-CSF therapy (20 μg/Kg/day) and his neutrophil count only recovered after allogeneic hematopoietic stem cell transplantation (HSCT). Two half-siblings of this patient, who were also diagnosed with SCN due to the same M1V mutation, did not respond to G-CSF therapy either (at a dose of 10 and up to 75 μg/kg/day), and also required HSCT (7, 8). ATA-P2 was a female diagnosed with SCN in the first year of life. She had been treated off and on with recombinant G-CSF throughout her life, with poor response and no evidence of cycling. While receiving maximal tolerable dosing of G-CSF on a daily weekday regimen (Monday through Friday), her total white blood cell count reached up to ~2,600 per mm^3, with absolute neutrophil count (ANC) of 234 per mm^3 and absolute monocyte count (AMC) of 832 per mm^3.

To study if the *ELANE* translation initiation codon mutation is sufficient and necessary to induce SCN pathogenesis, we additionally generated isogenic knock-in (GTG-KI), where we introduced the mutation c.1A>G in healthy donor (normal) iPSC and we corrected the mutation in GTG-P1 (SCN patient-derived iPSC line), named as GTG-C iPSC line (Supplementary Figure 1A). The patient-derived and knock-in iPSC lines retained the mutation c.1A>G, while CRIPSR/Cas9 mediated homology directed repair (HDR) led to correction of the heterozygote mutation in the GTG-C iPSC line (Supplementary Figure 1B). All iPSC lines maintained pluripotency and normal karyotype throughout the culture period (Supplementary Figures 1C-D).

iPSC lines were subjected to directed hematopoietic differentiation and generated similar levels of hematopoietic progenitors ($CD45^+CD34^+$) between isogenic iPSC lines, and the majority of these cells express CD43, a marker for primitive hematopoiesis (Supplementary Figures 2A-B). Hematopoietic progenitors from iPSC lines were cultured in ex-vivo granulopoiesis conditions (10) (Figure 1B). The growth of CD34-negative neutrophil precursors in ex-vivo granulopoiesis starting from mutation knock-in (GTG-KI) and patient-generated (GTG-P1) iPSC were reduced by ~75% and ~50%, respectively, compared to normal control **(**Figure 1C**).** The reduced cell growth was associated with increased apoptosis (Figure 1D and Supplementary Figures 3A-B), similar to other models of mutations in *ELANE* (10, 13). Gene correction of GTG-P1 iPSCs (GTG-C) restored cell growth and survival to levels comparable to normal iPSC derived precursors (Figure 1C and Supplementary Figures 3A-B). To examine whether SCN patient iPSC derived granulocytic precursors recapitulate the disease observed in SCN patients, we performed assays of in vitro directed granulopoiesis in the presence of G-CSF at low (50 ng/mL) and high (1000ng/mL) concentration, as described earlier (10), which roughly corresponds to peak plasma concentrations of G-CSF in infants receiving 1 or 20 μg/Kg/day respectively (14). During G-CSF directed granulopoiesis, cultures of *ELANE* c.1A>G **neutrophil precursors contained fewer cells** (Figure 1E) and had increased apoptosis both at low and high concentrations of G-CSF (Figure 1F). The granulocytic differential count of mutation knock-in (GTG-KI) and patient (GTG-P1) iPSC derived myeloid precursors was shifted left with significantly reduced levels of mature neutrophils ($CD45^+CD14^-CD11b^+CD15^+CD66b^+$) in both low and high levels of G-CSF, as assessed by flow cytometry (mature neutrophils: $CD45^+CD14^-CD11b^+CD15^+CD66b^+$) (Supplementary Figures 3C-E) and by morphological analysis (Figures 1G-H). High concentration of G-CSF did not ameliorate the defects in granulopoietic differentiation from the GTG-KI and GTG-P1 lines (Supplementary Figures 3F-G). These data suggest that *ELANE*-mutant SCN iPSC–derived myeloid precursor cells are arrested at the myelocyte stage of granulopoietic development even at supra-pharmacological concentrations of G-CSF. Survival and granulocytic maturation were restored to normal levels in

mutation corrected (GTG-C) neutrophil precursors (Figures 1D-H, Supplementary Figures 3C-G) without affecting the surface expression of CSF3R (Supplementary Figure 3H). Analysis of two other clones of healthy donor, mutant, knock-in, and corrected iPSC derived hematopoietic progenitors ($CD45^{+}CD34^{+}CD43^{+}$) (Supplementary Figures 4 A-B; Supplementary Figures 5A-C), further supported these findings and the effect of the translation initiation codon mutation on granulopoiesis failure both at low and high concentration of G-CSF (Supplementary Figures 5A-C; Supplementary Figures 6A-D). These results, taken together, demonstrate that *ELANE* translation initiation codon mutation is necessary and sufficient to recapitulate human SCN pathogenesis characterized by maturation arrest, cell death, and G-CSF resistance.

Neutrophil precursors with *ELANE* c.1A>G mutation express N-terminal truncated NE protein which aggregates and induce apoptosis preferentially via aggrephagy rather than UPR/ER stress like most other *ELANE* mutations.

To determine whether start-codon mutant ELANE resulted in a loss of the N-terminus of NE, we compared immunoblots using an antibody specific against the C-terminus region of NE (Supplementary Figure 7A-B) and a specific antibody directed against the amino-terminus of NE (Figure 2A). Consistent with our earlier report (12), neutrophil precursors ($CD45^{+}CD34^{-}CD11b^{-}CD14^{-}CD15^{+}$) derived from *ELANE* translation initiation codon mutant (GTG-KI and GTG-P1) iPSC expressed N-terminal truncated low molecular weight alternate NE (NE^{ALT}) and higher molecular weight NE bands possibly due to misfolding and aggregation (NE^{AGR}) of the truncated alternate NE (Figures 2A-B). As expected, cellular NE distribution was altered in mutant neutrophil precursors (12). While NE was predominantly cytoplasmic in healthy-donor and genetically corrected neutrophil precursors, most neutrophil precursors (~60%) displayed a predominantly nuclear distribution of NE (Supplementary Figures 7C-D). Healthy donor (Normal) and mutation corrected (GTG-C) neutrophil precursors predominantly expressed full-length NE (NE^{Normal}) (Figures 2A-B, Supplementary Figures 8A-B). A similar pattern of low molecular weight and aggregated forms of NE was observed in neutrophil precursors from ATA-P2 iPSC line carrying translation initiation codon mutation c.3G>A

mutation (Supplementary Figure 8C). Non-mutant NE or *ELANE*-exon 3 (*ELANE*$^{EX-3}$) missense mutations (NE^{I118N} and NE^{Q96P}) SCN patient iPSC-derived neutrophil precursors did not express NE^{ALT} and NE^{AGR} (Supplementary Figure 8D) suggesting a phenomenon specific to translation initiation codon mutations. Of note, no significant changes in the expression of BAG3 (Bcl2 associated athanogene-3), a co-chaperone critical for the aggrephagy of misfolded proteins (15), were associated with the presence of the *ELANE* translation initiation codon mutation (Figure 2B).

To determine if the high molecular weight bands detected by immunoblotting with anti-NE C-terminal region-specific antibody are indeed aggregated forms of mutant NE, we performed cell fractionation using ultracentrifugation (200,000g) to separate insoluble and aggregated proteins from supernatant containing soluble proteins. Fractionation of GAPDH exclusively in the supernatant fraction suggests that native proteins remain in the soluble fraction at 200,000g (Figure 2C). As shown in Figures 2C-D, NE and BAG3 from GTG-KI and GTG-P1 iPSC derived cells were highly insoluble and predominantly present in the pellet fractions. While pellet anti-BAG3 recognized a single band, pellet anti-NE recognized multiple high molecular weight bands. As expected, most NE from normal and mutation corrected granulocytic precursors was enriched in the supernatant fraction (Figures 2C-D). BAG3 was enriched in the pellet fractions of mutation carrying cells, but not in healthy or corrected cells (Figures 2C-D), further supporting the notion of induced aggrephagy in GTG-KI and GTG-P1 granulocyte precursors. The presence of NE-containing aggregates in *ELANE* translation initiation codon mutant, but not in normal or mutation corrected, neutrophil precursors was further confirmed by microscopy that demonstrated cytosolic co-localization of NE with the fluorescent dye ProteoStat (Figures 2E-F, Supplementary Figures 9A-B), a fluorescent molecular rotor that detects misfolded and aggregated proteins (16, 17).

Unlike *ELANE* $^{EX-3}$ mutations (10), neutrophil precursors cell death induced by *ELANE* c.1A>G mutation did associate with increased expression of pro-apoptotic BH3-only molecules (Supplementary Figure 10A) but did not associate consistently with increased UPR/ER stress

response (Supplementary Figure 10B). Intrigued by the lack of noticeable UPR/ER stress response, which was in clear contradiction with the behavior of other *ELANE* mutations (2, 10, 11), we hypothesized that an alternative cell death mechanism was at play. The aggregation of alternate NE peptides (Figures 2A-F, Supplementary Figures 8C and 9A-B) was associated with enriched distribution of BAG3 into the pellet fraction and increased expression of autophagic LC3B (Supplementary Figures 10C-D). Together, these data were strongly suggestive of the existence of aggrephagy activation in *ELANE* translation initiation codon mutant (GTG-KI, GTG-P1 and ATA-P2) neutrophil precursors. To further validate the induction of aggrephagy in mutant precursors, we analyzed the level of expression of the Bcl2 associated athanogene (BAG) family proteins that act as co-chaperones of HSP70 family proteins (18, 19). The existence of aggrephagy activation in GTG-KI and GTG-P1 mutant myeloid precursors was further supported by decreased BAG1L/BAG3 and BAG1S/BAG3 ratios, a hallmark of aggrephagy pathway activation, and BAG3 interaction with NE^{AGR} in mutant cells, as demonstrated by proximity ligation analysis (Figures 2G-J). We also found that the expression of all three isoforms of BAG1 (BAG1L, BAG1M and BAG1S) were drastically reduced in GTG-KI and GTG-P1 neutrophil precursors (Figure 2I). Gene editing mediated correction of the translation initiation codon mutation restored the expression of BAG1L, and to a lesser degree for BAG1S, to normal or close-to-normal precursor expression levels (Figure 2I). BAG1 and BAG3 act as co-chaperones (18, 19) driving, respectively, the misfolded protein response towards proteasome-mediated degradation (20) or the macroautophagic process of aggrephagy (15, 21). Therefore, the BAG1 to BAG3 protein ratio dictates a proteasome to autophagy switch in neurodegenerative diseases (22-24) and has been shown to be critical for HSC homeostasis and aging (25). The reduced expression of BAG1 isoforms, decreased BAG1/BAG3 ratio and association of BAG3 with NE supports our hypothesis of alternate NE peptide induced aggrephagy machinery in these cells, a mechanism similar to neurodegenerative diseases (24).

SERF1 is required for aggrephagy-induced cell death and G-CSF resistance of *ELANE* translation initiation mutant neutrophil precursors.

To understand the underlying mechanisms of aggrephagy-induced cell death and granulopoiesis arrest, we first examined the expression of known cellular chaperones. We found no change in the expression of heat shock proteins HSP90, HSP70, and HSP40, chaperones that regulate protein refolding to native states (Supplementary Figure 11A). The expression of SERF1A protein, known to regulate aggregation and proteotoxicity in neurodegenerative diseases (26-28), was significantly upregulated in *ELANE* c.1A>G, but not in *ELANE* $^{EX-3}$ mutant, neutrophil precursors (Figures 3A-B). SERF1 is an evolutionarily conserved human homologue of *C. elegans* MOAG4 protein (26) and regulates protein aggregation and age-related proteotoxicity (26-28). SERF1 is a nuclear stabilizer with capacity to bind RNA that translocates to the cytoplasm in response to stress generated by cytotoxic aggregates of misfolded proteins and bind to insoluble protein aggregates (29). As expected, we found SERF1 expression to be predominantly nuclear in normal and mutation corrected iPSC derived neutrophil precursors (Figure 3C). The increased SERF1 expression in *ELANE* translation initiation codon mutant (GTG-KI and GTG-P1) neutrophil precursors was associated with both nuclear and cytoplasmic distribution (Figures 3C-E). Consistent with our earlier report (12), we found NE located in both cytoplasm and nucleus of granulocyte precursors (Figure 3C). Proximity analysis between SERF1 and NE demonstrated that both proteins located in proximity in the cytoplasm of GTG-KI and GTG-P1 neutrophil precursors but not in healthy control or mutation-corrected cells (Figures 3F-G). Although we observed NE localization to the nucleus, we found no proximity between NE and SERF1 in the nucleus, suggesting that SERF1 did not interact with NE in the nucleus (Figures 3F-G). As a control for specificity, the endogenous protease inhibitor α1-anti trypsin (AAT) was found to interact with NE in all the groups tested (Supplementary Figure 11B) but not with SERF1 (Supplementary Figure 11C), reinforcing the notion that the interaction between SERF1 and NE is specific and distinct from other known interactions in neutrophil precursors (30).

To determine if SERF1 upregulation is essential for NE aggregation and SCN pathogenesis, we downregulated SERF1 expression using short hairpin RNA (Supplementary Figure 12A-D).

Downregulation of SERF1A rescued the survival (Figure 4A, Supplementary Figure 12E), differentiation, and G-CSF sensitivity of GTG-KI and GTG-P1 neutrophil precursors (Figure 4B-C), suggesting that downregulation of SERF1 made the *ELANE* translation initiation codon mutant neutrophil precursors sensitive to G-CSF, even at lower concentration (10). Mechanistically, SERF1 downregulation led to reduced levels of protein aggregates (Figures 4D-E). The reduced levels of protein aggregates and aggrephagy were confirmed by a decreased association of mutant NE with BAG3 (Figure 4F-G) and increased expression of BAG1 and its association with NE (Figure 4H-K). High-dose G-CSF therapy rescues *ELANE*-exon 3 ($ELANE^{EX\text{-}3}$) missense mutant granulopoiesis through c/EBPβ (2, 10). c/EBPβ is required for ApoE-dependent aggregate formation and aggrephagy in neurodegeneration (31). We hypothesized that aggrephagy activation results in autophagy induced cell death and its inhibition would allow G-CSF dependent c/EBPβ rescue of granulopoiesis. We found that silencing of SERF1 shifted the balance from G-CSF resistant aggrephagy towards G-CSF sensitive proteasome-mediated clearance of misfolded proteins. These results illustrate protein aggregation-mediated pathobiology of a hematopoietic disorder (Supplementary Figure 12F) and provide support to the notion of targeting aggrephagy pathways as an alternate therapeutic option for G-CSF resistant SCN.

Discussion

Severe congenital neutropenia (SCN) is frequently associated with dominant point mutations in *ELANE*, encoding neutrophil elastase (NE). *ELANE* mutant neutrophil precursors show aberrant distribution of NE, with accumulation in the ER and intracellular juxtamembrane regions. Unfortunately, animal modeling of mutant *ELANE* has been hampered by the fact that knock-in mice fail to phenocopy human disease (11, 32).

Our understanding of the pathobiology of mutant *ELANE* SCN has advanced in the last 10 years using gene edited human stem cell derived granulopoiesis (10, 13, 33). iPSCs derived from patients and healthy donors have been used to decipher pathogenetic mechanisms and for drug discovery (34-36). Others and we have used iPSC to unravel mechanisms of SCN pathogenesis (10, 12, 13, 37, 38). The generation and analysis of hematopoiesis derived from iPSC lines afford the efficient use of high-fidelity tools of gene editing resulting in bona-fide generation and repair of missense mutations through the preferential use of homology-directed repair (HDR) recombination (10). Using CRISPR/Cas9 gene-edited iPSC lines, our group earlier reported that *ELANE* missense mutations are necessary and sufficient to induce SCN pathogenesis (10). We also demonstrated that missense mutations in the exon 3 of *ELANE* induce neutropenia that can be ameliorated by G-CSF through alternative activation of *CEBPB* dependent granulopoiesis, as shown in primary myelopoiesis from patients (39, 40). Our group has previously demonstrated that mutations in the translation initiation codon of *ELANE*, a mutation associated with resistance to G-CSF administration (6-8), result in neutropenia, through the expression of alternative, truncated, misfolded peptides by cistrons initiated by alternative translation start codons and internal ribosomal entry sites (12). In this manuscript, we confirmed that *ELANE* start codon mutated neutrophil precursors express N-terminal truncated alternate NE and found that are specifically rich in the presence of cytosolic NE aggregates. Unlike G-CSF sensitive *ELANE* mutations that induce endoplasmic reticulum and unfolded protein response stress (10), we found that the mutation of the *ELANE* translation initiation codon resulted in an alternative pro-apoptotic pathway rather than the well described ER/UPR

stress response. This alternative pathway is the macroautophagic process of aggrephagy. While *ELANE* translation initiation codon mutations did not turn out into significant ER/UPR stress response and resulted in predominant nuclear localization of NE, we found downregulated BAG1 expression, increased BAG3/BAG1 ratio, co-localization of NE-aggregates in the cytoplasm with BAG3, and localized expression of autophagic LC3B. BAG1 and BAG3 act as co-chaperones (18, 19) driving, respectively, the misfolded protein response towards proteasome-mediated degradation (20) or the macroautophagic process of aggrephagy (15, 21). The existence of larger misfolded NE peptides in *ELANE* translation initiation mutations is the basis of the preferential defect. Our data clearly support that alternate, truncated NE protein induce the aggrephagy machinery in these cells, a mechanism similar to those ones resulting in neural and glial apoptosis in neurodegenerative diseases (24).

After ruling out a differential expression of HSP70 chaperone family proteins, we found that RNA-chaperone protein SERF1, known to induce misfolded protein aggregates in neurodegenerative diseases, is upregulated in the translation initiation codon $ELANE^{mut}$ neutrophil precursors, translocates to cytoplasm, and interacts with the truncated NE protein aggregates. Silencing of SERF1 enhanced survival and differentiation of iPSC-derived neutrophil precursors rendering them sensitive to G-CSF.

Chronic administration of granulocyte colony-stimulating factor (G-CSF) is a first-line treatment of *ELANE* mutant SCN. Unfortunately, patients with mutations near the N-terminus of the *ELANE* gene involving the translation initiation codon are resistant to G-CSF administration (6-8), having only HSCT as an available therapy. Given the early age of these patients when receiving HSCT and the large number of co-morbidities including bacterial and fungal infections, the mortality of these patients undergoing stem cell transplantation is very high. Chronic G-CSF therapy, even in responding patients, is not deprived of harmful consequences. Up to a quarter of *ELANE* mutant SCN cases on long-term, moderate/high-dose G-CSF therapy develop somatic CSF3R activating mutations preceding the onset of MDS/AML (9), underscoring the need to investigate alternative therapies that could decrease therapeutic reliance on G-CSF. We have previously demonstrated

that the addition of the NE inhibitor sivelestat to G-CSF improves the sensitivity of exon-3 missense mutations of ELANE to G-CSF, aiming to reduce the dose needed to generate granulopoietic responses to G-CSF (10).

In this manuscript, we now demonstrate that interference of the process of aggregation of misfolded truncated NE peptides prevents aggrephagy-induced apoptosis and restores G-CSF sensitivity of otherwise highly-resistant neutrophil precursors. Specifically, downregulation of SERF1, a major regulatory chaperone of misfolded protein aggregation and age-related proteotoxicity (26-28) which specifically locates in NE aggregates, completely prevents the need of high-dose G-CSF to induce granulopoiesis.

Our data support the presence of alternative mechanisms of apoptosis which depend on the specific location of each missense mutation. Our work provides an alternate therapeutic option for granulocyte recovery in SCN patients by using lower doses of G-CSF in combination with approaches to downregulate or degrade SERF1, and thereby decreasing the risk of these patients to develop secondary MDS and AML.

Materials and Methods

Sex as a biological variant

Male and female derived iPSC were used in this study. Sex was not considered as a biological variable since causal heterozygote mutations in *ELANE* are equally affecting males and females.

Human iPSC generation from healthy donor (normal) and *ELANE* translation initiation codon mutant SCN patient peripheral blood mononuclear cells (PB MNC)

iPSC lines, ”Normal” (from healthy donors) and SCN patients with heterozygous mutation at *ELANE* translation initiation codon [*ELANE* c.1A>G, p.(M1V) and *ELANE* c.3G>A, p.(M1I)] were generated with lentiviral vectors and characterized as described previously(10, 41). Once derived, iPSC lines were cultured on Matrigel (354277, Corning) and maintained with mTeSR1 medium (85850, StemCell Technologies).

Cell lines

RBL-1 cells were obtained from the American Type Culture Collection (ATCC) inventory (Manassas, VA).

Commercial sources of antibodies and fluorochrome-bound proteins

Antibody	Catalog	Manufacturer
V450 Mouse anti Human CD45, Clone HI30	560367	BD Horizon
APC/Cy7 anti-human CD34, clone 581	343514	BioLegend
FITC mouse anti Human CD43	555475	BD Pharmingen
APC/Cy7 Mouse anti Human CD11b	557754	BD Pharmingen
PE Mouse anti Human CD15	555402	BD Pharmingen
PerCP-Cy5.5 Mouse anti Human CD66b	562254	BD Pharmingen
PE-Cy7 mouse anti-Human CD14	560919	BD Pharmingen
anti NE antibody	OAAB08326	Aviva System Biology
anti ATT antibody (B9)	sc-59438	Santa Cruz Biotechnology
SERF1A	LS-C180169	LSBio
Anti-SERF1A	ARP67287_P050	Aviva System Biology
BAG1	ab32109	abcam
BAG3	ab47124	abcam

LC3B	ab192890	abcam
HSP70	4872	Cell Signalling Technologies
HSP90	4874	Cell Signalling Technologies
HSP40	4868	Cell Signalling Technologies
BAX	41162	Cell Signalling Technologies
BAK	3814	Cell Signalling Technologies
pBAD (S136)	4366	Cell Signalling Technologies
HRP-Goat anti-Chicken IgY	H-1004	Aves Labs, Inc.
HRP-anti Rabbit IgG	7074	Cell Signalling Technologies
HRP-anti Mouse IgG	7076	Cell Signalling Technologies
Alexa Fluor 568 Goat anti Chicken IgG	A11041	Life technologies
Alexa Fluor 488 Donkey anti Chicken IgY	703-545-1555	Jackson Immuno Research
Fluorochrome-bound proteins		
Annexin-V-APC	556454	BD Biosciences

Gene editing of *ELANE* translation initiation codon in iPSC lines

CRISPR/Cas9 gene editing technology was used to correct mutation (c.1A>G) in the *ELANE* patient iPSC line (GTG-P1) to generate the isogenic *ELANE* mutation corrected patient iPSC line (GTG-C). Human codon-optimized pX458 Cas9 plasmids were obtained from Addgene modified by CCHMC Transgenic Core as previously described(42). The Addgene Zhang's CRISPR designing tool (http://crispr.mit.edu/) was used to identify a single-guide RNA *ELANE* ATG (Assembly 2) to target *ELANE* exon 1 and cloned into the human codon-optimized pX459 Cas9 plasmid. The asymmetric donor plasmid was designed and synthesized by GenScript. *ELANE* CRISPR and asymmetric donor plasmids were purified. iPSC were cultured on 6 well Matrigel-coated dishes in mTeSR1 until confluence. Accutase (Sigma) was used to dissociate iPSC into single cells, and nucleofected with 1 µg each Assembly 2 CRISPR and 1 µg asymmetric donor construct using kit P3 and the Amaxa Nucleofector (Lonza). Cells were seeded on Matrigel-coated culture dishes after nucleofection, in mTeSR1 medium supplemented with 10 µM Y-27632 (Millipore). Cells were cultured for 2 days, dissociated into single cells using Accutase and the donor-expressing GFP+ iPSCs were sorted (Cincinnati Children's Flow Sorting facility) and plated onto Matrigel-coated culture dishes in mTeSR medium supplemented with 10uL ROCK inhibitor Y-27632. Selected clones/subclones with the

corrected gene edition were confirmed with Sanger sequencing and post-editing characterization was assessed.

The healthy donor iPSC line (Normal) was gene-edited using CRISPR/Cas9 method to knock in GTG mutation in place of translation initiation codon ATG of one allele of *ELANE* gene to generate isogenic knock-in iPSC line (GTG-KI). The same method and procedure that were used for the correction of mutation in the SCN patient derived iPSCs were followed except for using a different plasmid donor with GTG instead of ATG.

Hematopoietic and granulopoietic differentiation of healthy donor (normal), SCN patient, and isogenic mutation knock-in and corrected iPSCs

Directed hematopoietic differentiation of iPSCs was carried out using STEMdiff hematopoietic Kit (05310, StemCell Technologies) as per manufacturer's instruction. On day 12, floating $CD34^{+}CD45^{+}$ hematopoietic progenitors were harvested and cultured in myeloid expansion medium (IMDM+10% FBS) containing human SCF (50 ng/ml), human GM-CSF (10 ng/ml) and human IL-3 (10 ng/ml) for 5 days. Cells were counted, analyzed by flow cytometry and further cultured (5 days) in presence of G-CSF (50 ng/ml and 1000 ng/ml) for granulopoietic differentiation. At the end of granulopoietic differentiation, cells were evaluated for phenotypic and morphological granulopoietic differentiation using flow cytometry and Wright-Giemsa, respectively. The Wright-Giemsa-stained cells were scored morphologically for granulocytic precursor populations of promyelocytes, myelocytes, metamyelocytes, bands and neutrophils, as well as monocytes.

Flow cytometry, Immunophenotypic analysis, and cell sorting

For the analyses of directed hematopoietic differentiation, floating cells at day 12 of hematopoietic differentiation of iPSCs were harvested, washed and stained for human CD45, CD34 and CD43, and flow analyzed for the hematopoietic progenitors ($CD45^{+}CD34^{+}$). Cells at day12+5 in myeloid culture condition were analyzed for apoptosis using annexin V binding assay. Briefly, cells were labeled with antibodies against human CD45, CD34, CD14, CD11b,

CD15, and APC-annexin V at dilution of 1:100. Apoptosis of promyelocytes/myelocytes ($hCD45^{+}hCD34^{-}hCD14^{-}hCD11b^{-}hCD15^{+/dim}$) was evaluated by analyzing annexin V binding. Cells cultured in granulopoietic differentiation medium containing G-CSF (50 ng/ml and 1000 ng/ml) were flow analyzed for terminal granulopoiesis and monopoiesis (Neutrophils: $hCD45^{+}hCD14^{-}hCD11b^{+}hCD15^{+/hi}hCD66b^{+}$, Monocytes: $hCD45^{++}hCD14^{+}hCD11b^{+}$). For promyelocytes/myelocytes cell sorting, cells in myeloid culture conditions (Day12+5) were stained for human CD45, CD34, CD14, CD11b, CD15, and promyelocytes/myelocytes ($hCD45^{+}hCD34^{-}hCD14^{-}hCD11b^{-}hCD15^{+/dim}$) were FACS sorted, and used for RNA extraction, immunoblots and confocal immunofluorescence microscopy. FACS-Canto flow cytometer (BD Biosciences) and the FACSAria II cell sorter (BD Biosciences) were used for analyses and cell sorting, respectively.

Quantitative RT-PCR

Total RNA was extracted from FACS sorted Normal Control, GTG-KI, GTG-P1 and GTG-C neutrophil precursors using RNeasy minikit (QIAGEN; catalog 74104) following manufacturer's instructions, and cDNA was prepared using Taq Man reverse transcription reagent (Applied Biosystems, Life technologies, catalog N8080234). The mRNA expression levels of *XBP1s, HSPA5, ATF6* and *DDIT3* were analyzed by Q-RT-PCR assay using TaqMan Universal PCR master mix and gene specific TaqMan primers (Roche Applied Science, Life technologies). The expression level was normalized to the expression of internal control gene *GAPDH*.

Immunoblot analyses

Neutrophil precursors ($hCD45^{+}hCD34^{-}hCD14^{-}hCD11b^{-}hCD15^{+}$) were sorted from Normal Control, GTG-KI, GTG-P1 and GTG-C myeloid cultures. Sorted neutrophil precursors were lysed in RIPA buffer containing protease inhibitor cocktail (Roche, Catalog 04693159001) and phosphatase inhibitors (Roche, Catalog 046906837001). The whole cell lysates were dissolved in 2.1% SDS-containing Laemmli's buffer (final concentration of SDS was 1.05%) and boiled for denaturation. Lysates were electrophoresed through 4%–15% SDS-PAGE gradient gel followed

by transfer to PVDF membrane. To separate insoluble aggregates and soluble protein fractions, neutrophil precursors were lysed in buffer (50 mM Tris-HCl, PH=8.0 50 mM NaCl, 5 mM EDTA, 1% Triton-X-100 supplemented with protease inhibitor cocktail for 20 min on ice, without SDS. The lysate was cleared by centrifuging at 10,000g for 10 min at 4^0C followed by ultracentrifugation at 200,000g for 2 h. The pellet was resuspended in 100 μL lysis buffer and 100 μL 2x SDS-containing Laemmli buffer. Both pellet and supernatant fractions were processed for SDS-PAGE (4-15% gradient) and immunoblot analyses. The membranes were probed with primary antibodies against NE from immunized chicken (IgY, dilution 1:5000) (12) , BAX, BAK, p-BAD, HSP70, HSP40, HSP90p, SERF1, BAG1, BAG3 and β–ACTIN (dilutions 1:1000) followed by secondary antibodies tagged with HRP (anti–mouse IgG, anti-rabbit IgG or anti-Chicken IgY, dilution 1:5000). The blots were developed using a chemiluminescence coupled reaction. The band intensities on the X-ray films were quantitated by using ImageJ software and normalized against β-ACTIN band intensity of the corresponding sample.

Confocal immunofluorescence microscopy

Sorted neutrophil precursors (hCD45+hCD34-hCD14-hCD11b-hCD15+) from day10+5 myeloid culture were fixed (4% paraformaldehyde), permeabilized (0.1% TX-100), blocked (3% goat serum or 3% BSA), treated with primary antibodies against NE (specific for C-terminal region of NE, dilution 1:2000) (12), anti-NE antibodies (specific for N-terminal region of NE, dilution 1:100), LC3B (dilution 1:200), SERF1 (dilution 1:200) overnight at 4^0C. Cells were washed and stained using fluorochrome tagged secondary antibodies (dilution 1:500), washed and mounted with prolong gold antifade mounting media with DAPI (ThermoFisher Scientific, Cat#P36935) to counterstain the nuclei. For the single-cell quantification of nuclear NE distribution, cells with predominantly nuclear NE distribution were counted as those ones in which the nuclear mean fluorescence intensity (MFI) per surface area represented more than 50% of the cell NE associated fluorescence. For the visualization of protein (NE) aggregates, sorted Normal Control, GTG-KI, GTG-P1 and GTG-C iPSC neutrophil precursors were fixed 4% paraformaldehyde (15 min, RT), washed and permeabilized with PBS supplemented with 0.1%

TX-100, 0.03% Tween 20 and 1% BSA (15 min, RT). Cells were washed and blocked with PBS supplemented with 1% BSA and 0.03% Tween 20 (1 h, RT). Cells were treated with anti-NE antibody (Chicken IgY at 1:2000 dilution)(12) overnight at 4^0C. Cells were washed and incubated with Alexa Fluor 488 conjugated donkey anti-chicken IgY (1:500) and ProteoStat (Enzo, 1:2500) for 1 h at RT. Cells were washed, mounted with prolong gold antifade mounting media containing 1 μg/mL DAPI, and were analyzed using a LSM 710 confocal system (Zeiss) attached to an inverted microscope (Observer Z1, Zeiss) equipped with a Plan Apochromat × 63 1.4 NA oil immersion lens.

Proximity ligation assay (PLA) and confocal microscopy

Proximity ligation assay was performed to detect interaction of protein residing in close proximity or in a multi protein complex, as per manufacturer's instruction (Sigma-Aldrich; catalog DUO92002, DUO92004). Briefly, Normal Control, GTG-KI, GTG-P1 and GTG-C neutrophil precursors were cytospun onto superfrost plus microscope slide (Fisher Scientific), fixed using 4% paraformaldehyde, permeabilized with 0.1% Triton X-100 for 10 minutes followed by blocking with DuoLink Blocking solution. Cells were treated with primary antibodies against SERF1 and NE or BAG3 and NE or BAG1 and NE or AAT and NE or AAT and SERF1 overnight at 4^0C. Cells were washed, treated with rabbit and mouse secondary antibody coupled with nucleotide probes (DuoLink InSitu PLA probe α-Rabbit PLUS and DuoLink InSitu PLA probe α-mouse MINUS or DuoLink InSitu PLA probe α-rabbit PLUS and DuoLink InSitu PLA probe α-Goat MINUS) for 1 h at 37^0C. The probes were ligated together (30 min at 37^0C), hybridized to form a circular DNA. Fluorescent labeled oligonucleotides are then incorporated during the process of rolling-circle amplification (100 min at 37^0C). Cells were washed and mounted using prolong anti-fade mounting media containing DAP. The stained cells were analyzed using a LSM 710 confocal system (Carl Zeiss) attached to an inverted microscope (Observer Z1, Zeiss) equipped with a Plan Apochromat × 63 1.4 NA oil immersion lens.

Statistics

Data are presented as individual data and mean ± standard deviation of a minimum of three replicates per experiment and a minimum of two independent experiments. Statistically significant differences were assessed by Student's t-test for two independent variables or for analyses of more than two variables, by one-way or two-way ANOVA tests with Bonferroni correction.

Study approval

Peripheral blood from healthy donors and SCN patients carrying the *ELANE* start codon mutation (*ELANE* c.1A>G, *ELANE* c.3G>A) was obtained at Cincinnati Children's Hospital Medical Center through informed consent under an approved institutional review board research protocol.

Data availability

Supporting data values are presented in a supplementary data file. The authors declare that all data supporting the findings of this study are available, to the best of our effort, within this manuscript and supplementary information files, and will be available from the corresponding authors upon request. Human subject data will be available deidentified.

Acknowledgements

The authors wish to thank the families who provided specimens from their children afflicted of severe congenital neutropenia and the healthy donors who also provided deidentified specimens for the generation of induced pluripotent stem cells. The authors wish to thank the Viral Vector Core of the Translational Core Laboratories of Cincinnati Children's Hospital Medical Center, supported by the NIDDK Center of Excellence in Hematology grant U54 DK126108. This project was also funded by grants from the NIDDK DK124115 and NHLBI P01HL158688.

Author contribution statement

RCN, SE, LRT, AMW, BK and AKS performed experiments. KCM and TK generated clinical data. RCN, CML and JAC supervised the project and designed experiments. MSH generated reagents specifically for this study and generated clinical data. RCN and JAC interpreted data and wrote the manuscript. All authors contributed intellectually to the project and reviewed the manuscript.

Conflict-of-interest disclosure

The authors declare no conflicts of interest relevant to the content of this manuscript

References

1. Berliner N, Horwitz M, and Loughran TP, Jr. Congenital and acquired neutropenia. *Hematology / the Education Program of the American Society of Hematology American Society of Hematology Education Program.* 2004:63-79.
2. Horwitz MS, Corey SJ, Grimes HL, and Tidwell T. ELANE mutations in cyclic and severe congenital neutropenia: genetics and pathophysiology. *Hematol Oncol Clin North Am.* 2013;27(1):19-41, vii.
3. Dale DC, Person RE, Bolyard AA, Aprikyan AG, Bos C, Bonilla MA, et al. Mutations in the gene encoding neutrophil elastase in congenital and cyclic neutropenia. *Blood.* 2000;96(7):2317-22.
4. Horwitz M, Benson KF, Person RE, Aprikyan AG, and Dale DC. Mutations in ELA2, encoding neutrophil elastase, define a 21-day biological clock in cyclic haematopoiesis. *Nat Genet.* 1999;23(4):433-6.
5. Bonilla MA, Gillio AP, Ruggeiro M, Kernan NA, Brochstein JA, Abboud M, et al. Effects of recombinant human granulocyte colony-stimulating factor on neutropenia in patients with congenital agranulocytosis. *N Engl J Med.* 1989;320(24):1574-80.
6. Germeshausen M, Deerberg S, Peter Y, Reimer C, Kratz CP, and Ballmaier M. The spectrum of ELANE mutations and their implications in severe congenital and cyclic neutropenia. *Hum Mutat.* 2013;34(6):905-14.
7. Setty BA, Yeager ND, and Bajwa RP. Heterozygous M1V variant of ELA-2 gene mutation associated with G-CSF refractory severe congenital neutropenia. *Pediatr Blood Cancer.* 2011;57(3):514-5.
8. Hashem H, Abu-Arja R, Auletta JJ, Rangarajan HG, Varga E, Rose MJ, et al. Successful second hematopoietic cell transplantation in severe congenital neutropenia. *Pediatr Transplant.* 2018;22(1).
9. Rosenberg PS, Alter BP, Bolyard AA, Bonilla MA, Boxer LA, Cham B, et al. The incidence of leukemia and mortality from sepsis in patients with severe congenital neutropenia receiving long-term G-CSF therapy. *Blood.* 2006;107(12):4628-35.
10. Nayak RC, Trump LR, Aronow BJ, Myers K, Mehta P, Kalfa T, et al. Pathogenesis of ELANE-mutant severe neutropenia revealed by induced pluripotent stem cells. *J Clin Invest.* 2015;125(8):3103-16.
11. Nanua S, Murakami M, Xia J, Grenda DS, Woloszynek J, Strand M, et al. Activation of the unfolded protein response is associated with impaired granulopoiesis in transgenic mice expressing mutant Elane. *Blood.* 2011;117(13):3539-47.
12. Tidwell T, Wechsler J, Nayak RC, Trump L, Salipante SJ, Cheng JC, et al. Neutropenia-associated ELANE mutations disrupting translation initiation produce novel neutrophil elastase isoforms. *Blood.* 2014;123(4):562-9.
13. Nasri M, Ritter M, Mir P, Dannenmann B, Aghaallaei N, Amend D, et al. CRISPR/Cas9-mediated ELANE knockout enables neutrophilic maturation of primary hematopoietic stem and progenitor cells and induced pluripotent stem cells of severe congenital neutropenia patients. *Haematologica.* 2020;105(3):598-609.
14. Yang BB, Kido A, and Shibata A. Serum pegfilgrastim concentrations during recovery of absolute neutrophil count in patients with cancer receiving pegfilgrastim after chemotherapy. *Pharmacotherapy.* 2007;27(10):1387-93.
15. Gamerdinger M, Kaya AM, Wolfrum U, Clement AM, and Behl C. BAG3 mediates chaperone-based aggresome-targeting and selective autophagy of misfolded proteins. *EMBO Rep.* 2011;12(2):149-56.
16. Cheng S, Banerjee S, Daiello LA, Nakashima A, Jash S, Huang Z, et al. Novel blood test for early biomarkers of preeclampsia and Alzheimer's disease. *Sci Rep.* 2021;11(1):15934.
17. Jash S, Banerjee S, Cheng S, Wang B, Qiu C, Kondo A, et al. Cis P-tau is a central circulating and placental etiologic driver and therapeutic target of preeclampsia. *Nat Commun.* 2023;14(1):5414.

18. Takayama S, and Reed JC. Molecular chaperone targeting and regulation by BAG family proteins. *Nat Cell Biol.* 2001;3(10):E237-41.
19. Briknarova K, Takayama S, Brive L, Havert ML, Knee DA, Velasco J, et al. Structural analysis of BAG1 cochaperone and its interactions with Hsc70 heat shock protein. *Nat Struct Biol.* 2001;8(4):349-52.
20. Luders J, Demand J, and Hohfeld J. The ubiquitin-related BAG-1 provides a link between the molecular chaperones Hsc70/Hsp70 and the proteasome. *J Biol Chem.* 2000;275(7):4613-7.
21. Meriin AB, Narayanan A, Meng L, Alexandrov I, Varelas X, Cisse, II, et al. Hsp70-Bag3 complex is a hub for proteotoxicity-induced signaling that controls protein aggregation. *Proc Natl Acad Sci U S A.* 2018;115(30):E7043-E52.
22. Gamerdinger M, Hajieva P, Kaya AM, Wolfrum U, Hartl FU, and Behl C. Protein quality control during aging involves recruitment of the macroautophagy pathway by BAG3. *EMBO J.* 2009;28(7):889-901.
23. Minoia M, Boncoraglio A, Vinet J, Morelli FF, Brunsting JF, Poletti A, et al. BAG3 induces the sequestration of proteasomal clients into cytoplasmic puncta: implications for a proteasome-to-autophagy switch. *Autophagy.* 2014;10(9):1603-21.
24. Rubinsztein DC. The roles of intracellular protein-degradation pathways in neurodegeneration. *Nature.* 2006;443(7113):780-6.
25. Chua BA, Lennan CJ, Sunshine MJ, Dreifke D, Chawla A, Bennett EJ, et al. Hematopoietic stem cells preferentially traffic misfolded proteins to aggresomes and depend on aggrephagy to maintain protein homeostasis. *Cell Stem Cell.* 2023;30(4):460-72 e6.
26. van Ham TJ, Holmberg MA, van der Goot AT, Teuling E, Garcia-Arencibia M, Kim HE, et al. Identification of MOAG-4/SERF as a regulator of age-related proteotoxicity. *Cell.* 2010;142(4):601-12.
27. Meinen BA, Gadkari VV, Stull F, Ruotolo BT, and Bardwell JCA. SERF engages in a fuzzy complex that accelerates primary nucleation of amyloid proteins. *Proc Natl Acad Sci U S A.* 2019;116(46):23040-9.
28. Merle DA, Witternigg A, Tam-Amersdorfer C, Hartlmuller C, Spreitzer E, Schrank E, et al. Increased Aggregation Tendency of Alpha-Synuclein in a Fully Disordered Protein Complex. *J Mol Biol.* 2019;431(14):2581-98.
29. Meyer NH, Dellago H, Tam-Amersdorfer C, Merle DA, Parlato R, Gesslbauer B, et al. Structural Fuzziness of the RNA-Organizing Protein SERF Determines a Toxic Gain-of-interaction. *J Mol Biol.* 2020;432(4):930-51.
30. Clemmensen SN, Jacobsen LC, Rorvig S, Askaa B, Christenson K, Iversen M, et al. Alpha-1-antitrypsin is produced by human neutrophil granulocytes and their precursors and liberated during granule exocytosis. *Eur J Haematol.* 2011;86(6):517-30.
31. Xia Y, Wang ZH, Zhang J, Liu X, Yu SP, Ye KX, et al. C/EBPbeta is a key transcription factor for APOE and preferentially mediates ApoE4 expression in Alzheimer's disease. *Mol Psychiatry.* 2021;26(10):6002-22.
32. Grenda DS, Johnson SE, Mayer JR, McLemore ML, Benson KF, Horwitz M, et al. Mice expressing a neutrophil elastase mutation derived from patients with severe congenital neutropenia have normal granulopoiesis. *Blood.* 2002;100(9):3221-8.
33. Rao S, Yao Y, Soares de Brito J, Yao Q, Shen AH, Watkinson RE, et al. Dissecting ELANE neutropenia pathogenicity by human HSC gene editing. *Cell Stem Cell.* 2021;28(5):833-45 e5.
34. Grskovic M, Javaherian A, Strulovici B, and Daley GQ. Induced pluripotent stem cells--opportunities for disease modelling and drug discovery. *Nature reviews Drug discovery.* 2011;10(12):915-29.
35. Gunaseeli I, Doss MX, Antzelevitch C, Hescheler J, and Sachinidis A. Induced pluripotent stem cells as a model for accelerated patient- and disease-specific drug discovery. *Current medicinal chemistry.* 2010;17(8):759-66.
36. Deng W. Induced pluripotent stem cells: paths to new medicines. A catalyst for disease modelling, drug discovery and regenerative therapy. *EMBO reports.* 2010;11(3):161-5.

37. Hiramoto T, Ebihara Y, Mizoguchi Y, Nakamura K, Yamaguchi K, Ueno K, et al. Wnt3a stimulates maturation of impaired neutrophils developed from severe congenital neutropenia patient-derived pluripotent stem cells. *Proc Natl Acad Sci U S A.* 2013;110(8):3023-8.
38. Morishima T, Watanabe K, Niwa A, Hirai H, Saida S, Tanaka T, et al. Genetic correction of HAX1 in induced pluripotent stem cells from a patient with severe congenital neutropenia improves defective granulopoiesis. *Haematologica.* 2014;99(1):19-27.
39. Skokowa J, and Welte K. Dysregulation of myeloid-specific transcription factors in congenital neutropenia. *Ann N Y Acad Sci.* 2009;1176:94-100.
40. Skokowa J, Cario G, Uenalan M, Schambach A, Germeshausen M, Battmer K, et al. LEF-1 is crucial for neutrophil granulocytopoiesis and its expression is severely reduced in congenital neutropenia. *Nat Med.* 2006;12(10):1191-7.
41. Salomonis N, Dexheimer PJ, Omberg L, Schroll R, Bush S, Huo J, et al. Integrated Genomic Analysis of Diverse Induced Pluripotent Stem Cells from the Progenitor Cell Biology Consortium. *Stem Cell Reports.* 2016;7(1):110-25.
42. Chen B, Gilbert LA, Cimini BA, Schnitzbauer J, Zhang W, Li GW, et al. Dynamic imaging of genomic loci in living human cells by an optimized CRISPR/Cas system. *Cell.* 2013;155(7):1479-91.

Figures

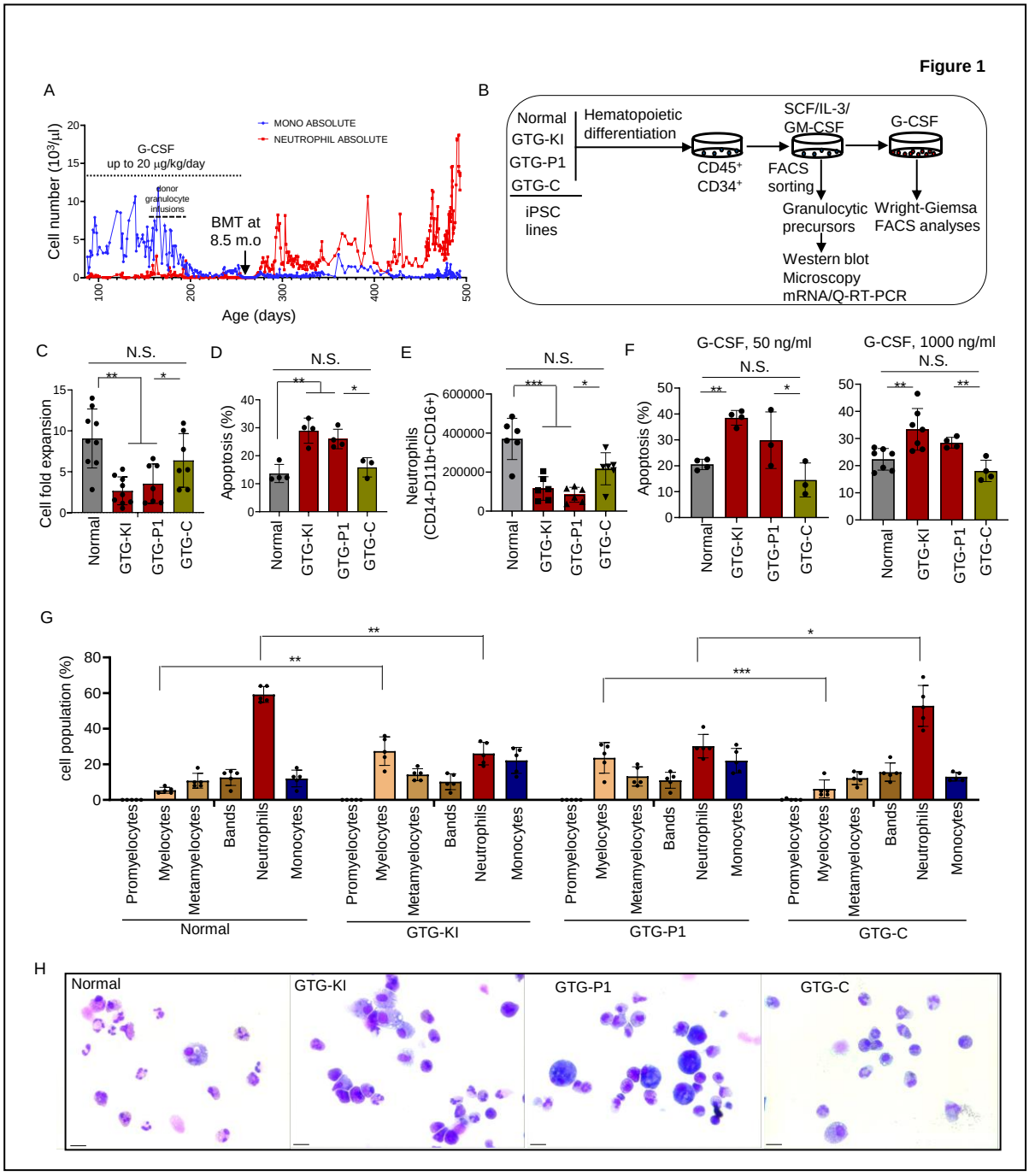

Figure 1. Neutrophil precursors with mutation at translation initiation codon (c.1A>G) of *ELANE* is associated with cell death, differentiation arrest and G-CSF resistance. A) PB ANC and AMC of a patient with *ELANE* translation initiation codon mutation (c.1A>G, NEp.M1V) from diagnosis at 3 months after birth up to 16 months. The patient was found to have leukopenia, severe neutropenia (ANC=0) and monocytosis (AMC=2720/mm^3). G-CSF

(20μg/Kg/day) administration showed minimal effect on ANC. Donor granulocyte transfusion did not increase neutrophil counts. This patient underwent allogeneic bone marrow transplantation resulting in ANC recovery. B) Experimental schema of modeling of SCN with *ELANE* translation initiation codon mutation employing directed hematopoietic and granulopoietic differentiation of normal (healthy donor iPSC*),* isogenic gene- edited GTG-KI (GTG Knock-in in place of ATG in one allele of *ELANE* gene of Normal iPSC), GTG-P1 (*ELANE* c.1A>G SCN patient derived iPSC), and GTG-C (correction of GTG to ATG in SCN patient GTG-P1 iPSC). C) Cell growth of normal, GTG-KI, GTG-P1, and GTG-C iPSC derived hematopoietic progenitors ($CD34^{+}CD45^{+}$). D) Quantification of the apoptosis of normal, GTG-KI, GTG-P1, and GTG-C neutrophil precursors ($CD45^{+}CD34^{-}CD14^{-}CD11b^{-}CD15^{+/dim}$). E) Flow cytometry analyses of the granulopoiesis (mature neutrophils: $CD45^{+}CD14^{-}CD11b^{+}CD16^{+}CD66b^{+}$) of normal, GTG-KI, GTG-P1 and GTG-C iPSC derived hematopoietic progenitors in presence of 50 ng/ml G-CSF. F) Quantification of the apoptosis of normal, GTG-KI, GTG-P1, and GTG-C neutrophil precursors ($CD45^{+}CD34^{-}CD14^{-}CD11b^{-}CD15^{+}$) in presence of 50 ng/mL and 1000 ng/ml G-CSF. G-H) Quantification (G) and representative morphological microphotographs (H) of output cells of G-CSF (50 ng/mL) induced differentiation of normal, GTG-KI, GTG-P1 and GTG-C iPSC derived hematopoietic progenitors (Wright-Giemsa staining; O.M. 40x). Data are presented as individual data and mean ± standard deviation of a minimum of three replicates per experiment and a minimum of two independent experiments. Comparison between groups was calculated using one way ANOVA. * $p<0.05$; ** $p<0.01$, *** $p<0.001$.

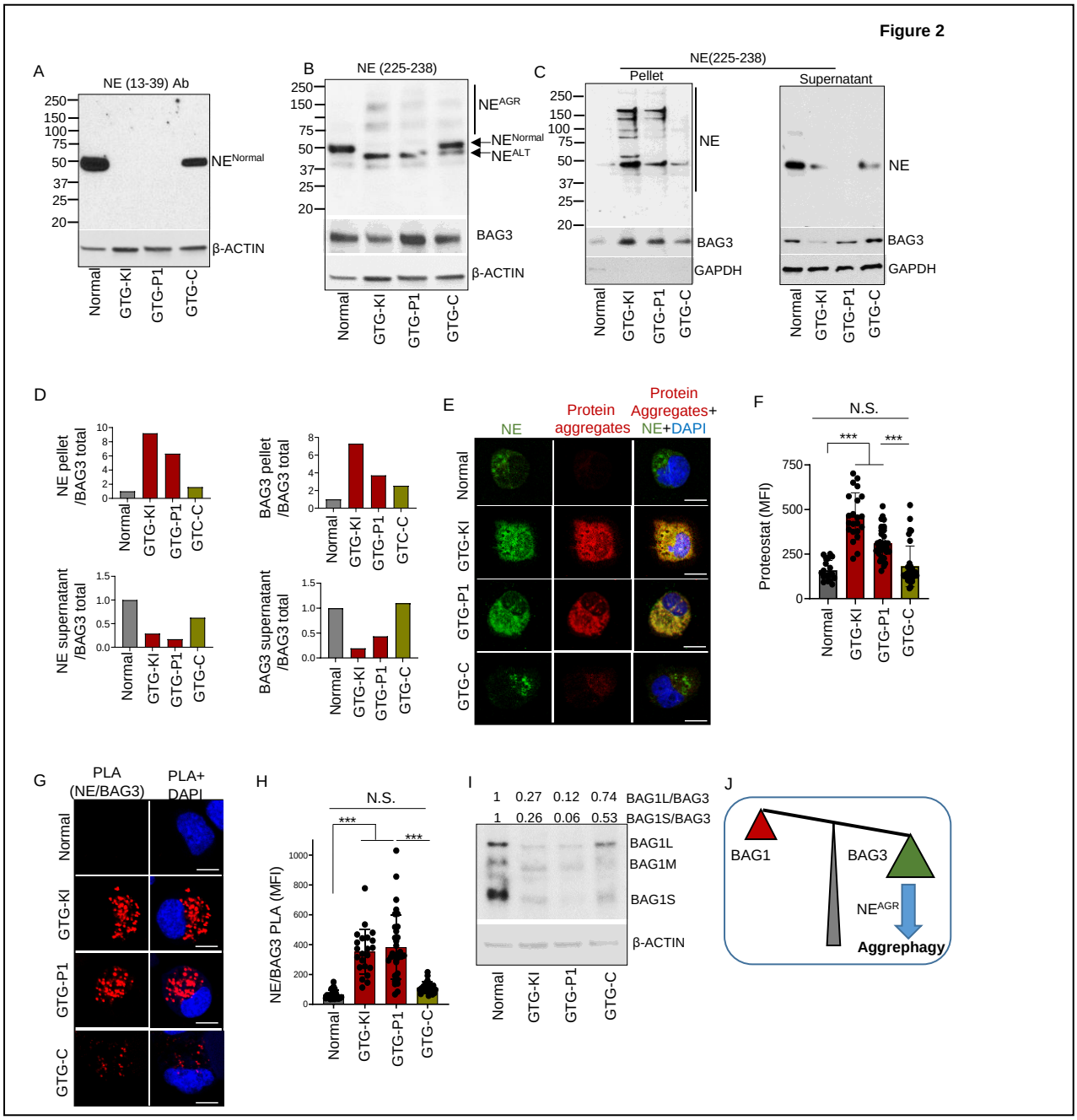

Figure 2. Neutrophil precursors with mutation at translation initiation codon of *ELANE* express low molecular weight alternate NE (NE^{ALT}), generates NE aggregates (NE^{AGR}) and induces aggrephagy. A) Representative immunoblot analyses of full- length NE (NE^{normal}) expression using α–NE Ab against N-terminal region (aa13-39) of NE. B) Representative immunoblot of NE expression in neutrophil precursors derived from normal, GTG-KI, GTG-P1 and GTG-C iPSC lines using an α–NE Ab against the C-terminal (aa225-238) region of the

protein. GTG-KI and GTG-P1 iPSC derived neutrophil precursors express alternate NE (NE^{ALT}) and possibly aggregates (NE^{AGR}) of alternate NE peptides, and mutation correction rescues full length NE expression. Some of the NE^{ALT} and NE^{AGR} expression in GTG-C line could be due to contamination of mutant iPSC cells during clonal isolation. C) Representative NE immunoblot in the pellet and soluble fraction of granulocyte precursors lysate ultracentrifugation. D) Quantification of NE and BAG3 in Figure 2C in pellets and soluble fractions and presented as a normalized ratio over BAG3 (from panel B). E) Representative confocal microscopic images of NE in association with ProteoStat fluorescent molecular rotor dye. F) MFI of ProteoStat stained aggresome. G) Representative immunoblots of BAG1 isoforms (BAG1L, BAG1M, and BAG1S) in normal, GTG-KI, GTG-P1 and GTG-C neutrophil precursors. H-I) Representative confocal microscopic images (H) and MFI (I) of proximity ligation assay (PLA) signal between NE and BAG3 in normal, GTG-KI, GTG-P1 and GTG-C neutrophil precursors. J) Schematic depiction of BAG3 and BAG1 protein ratio and association with alternate NE aggregation. Bar=10 μm. The mean fluorescence intensities of more than 10 cells from 2 independent experiments was quantified. Data are presented as individual data and mean ± standard deviation of two or three replicates per experiment and a minimum of two independent experiments. Comparison between groups was calculated using one way ANOVA. * $p<0.05$; ** $p<0.01$, *** $p<0.001$.

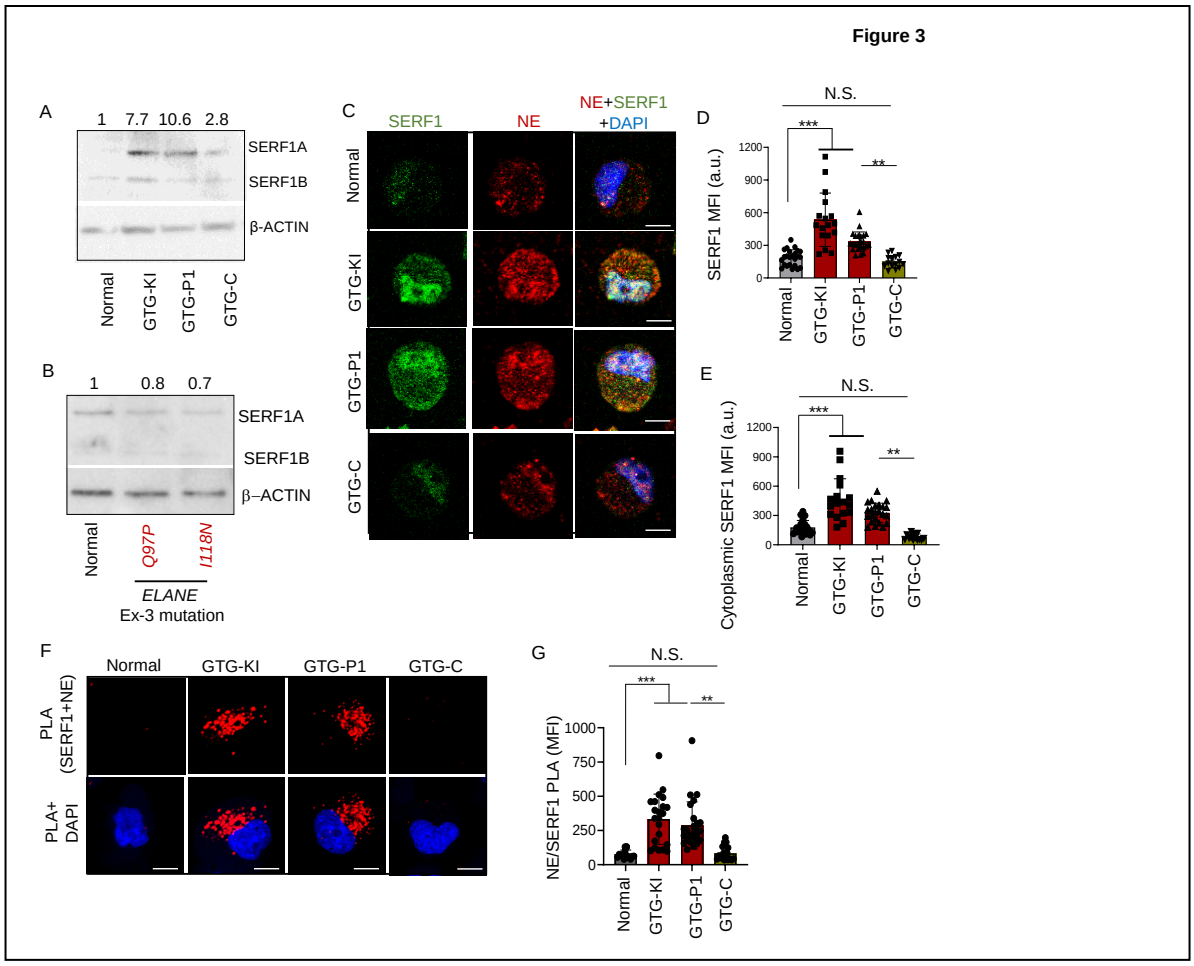

Figure 3. Expression of SERF1, an RNA binding chaperone, is upregulated and SERF1 interacts with NE aggregates in *ELANE* translation initiation codon mutant neutrophil precursors. A) Representative immunoblots of SERF1A and SERF1B in normal, GTG-KI, GTG-P1 and GTG-C neutrophil precursors. SERF1A, but not SERF1B, expression is upregulated in *ELANE* translation initiation mutant neutrophil precursors. B) Representative WBs of SERF1A and SERF1B in healthy donor (normal*), ELANE*$^{EX-3}$ *mutant* (I118N, Q97P) iPSC derived neutrophil precursors. SERF1A expression is marginally reduced in *ELANE* ex-3 mutant SCN. C-D) Representative confocal microscopic images of NE and SERF1 (C) and mean fluorescence intensities (D) of SERF1A in normal, GTG-KI, GTG-P1 and GTG-C neutrophil precursors. E) Quantification of SERF1 cytoplasmic expression in normal, GTG-KI, GTG-P1 and GTG-C neutrophil precursors. Increased SERF1 expression is associated with translocation to cytoplasm. F-G) Representative confocal images (F) and mean fluorescence intensities (G) of PLA signal between SERF1 and NE normal, GTG-KI, GTG-P1 and GTG-C

neutrophil precursors. Bar= 10 μm. The mean fluorescence intensities of more than 10 cells from 2 independent experiments was quantified. Data are presented as individual data and mean ± standard deviation of two or three replicates per experiment and a minimum of two independent experiments. Comparison between groups was calculated using one way ANOVA. * $p<0.05$; ** $p<0.01$, *** $p<0.001$.

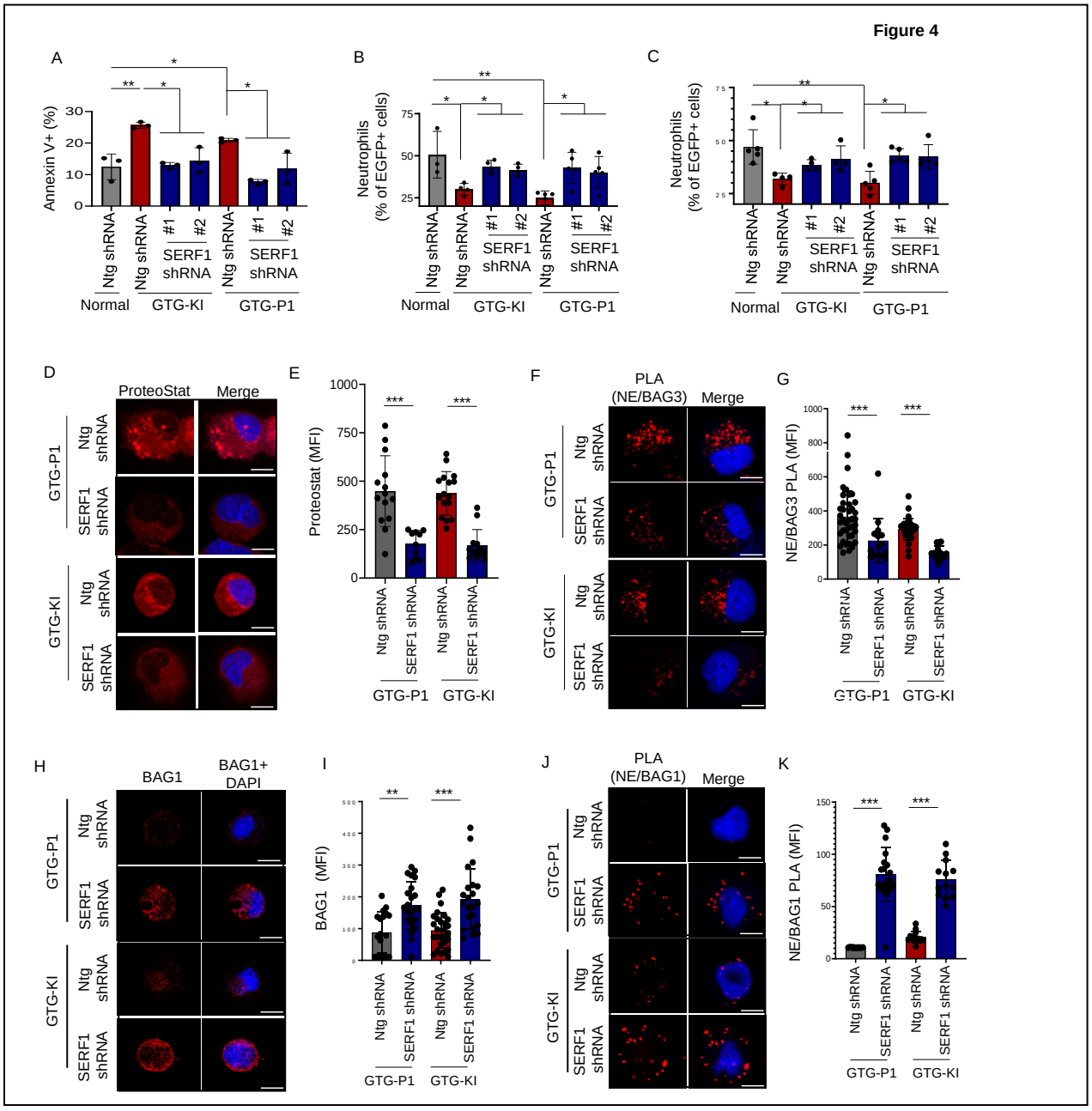

Figure 4. SERF1 downregulation restores survival and granulocytic differentiation of *ELANE* translation initiation codon mutant neutrophil precursors. A) Apoptosis of non-targeting (Ntg) shRNA and SERF1 shRNA transduced GTG-KI and GTG-P1 neutrophil precursors. SERF1 down regulation led to increased survival of GTG-KI and GTG-P1 neutrophil precursors. B) Granulopoietic differentiation of Ntg shRNA and SERF1 shRNA transduced GTG-KI and GTG-P1 iPSC lines derived hematopoietic progenitors at 50 ng/mL G-CSF. C) Granulopoietic differentiation of Ntg shRNA and SERF1 shRNA transduced GTG-KI

and GTG-P1 iPSC lines derived hematopoietic progenitors at 1000 ng/ml G-CSF. D-E) Representative confocal microscopic images (D) and mean fluorescence intensities (E) of ProteoStat fluorescent molecular rotor dye in Ntg shRNA and SERF1 shRNA transduced GTG-KI and GTG-P1 neutrophil precursors. F-G) Representative confocal microscopic images (F) and mean fluorescence intensities (G) of PLA signals between NE and BAG3 in Ntg shRNA and SERF1 shRNA transduced GTG-KI and GTG-P1 neutrophil precursors. H-I) Representative confocal microscopic images and mean fluorescence intensities of BAG1 expression in Ntg shRNA and SERF1 shRNA transduced GTG-KI and GTG-P1 neutrophil precursors. J-K) Representative confocal microscopic images and mean fluorescence intensities of PLA between NE and BAG1. SERF1 downregulation enhanced NE interaction with BAG1 in GTG-P1 and GTG-KI neutrophil precursors. Bar= 10 μm. The mean fluorescence intensities of more than 10 cells from 2 independent experiments was quantified. Data are presented as individual data and mean ± standard deviation of two or three replicates per experiment and a minimum of two independent experiments. Comparison between groups was calculated using one way ANOVA. * $p<0.05$; ** $p<0.01$, *** $p<0.001$.